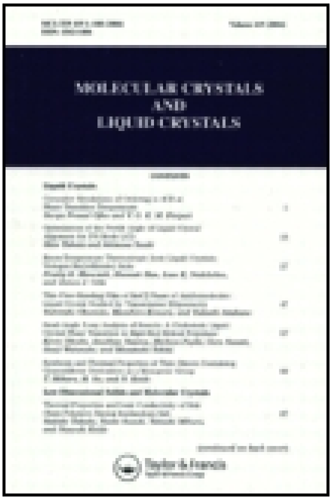

Molecular Crystals and Liquid Crystals
Publication details, including instructions for authors and subscription information:
http://www.tandfonline.com/loi/gmcl20

Synthesis and Physico-Chemical Properties for 2-Oxochromen-6-yl 4-(4-Alkoxyphenylazo)benzoates

Yuki Morita [a], Hiroshi Uemura [a], Kentaro Shimoi [a], Kazuo Kasatani [a] & Hiroaki Okamoto [a]
[a] Department of Advanced Materials Science and Engineering, Faculty of Engineering, Yamaguchi University, Ube, Yamaguchi, Japan

To cite this article: Yuki Morita, Hiroshi Uemura, Kentaro Shimoi, Kazuo Kasatani & Hiroaki Okamoto (2009) Synthesis and Physico-Chemical Properties for 2-Oxochromen-6-yl 4-(4-Alkoxyphenylazo)benzoates, Molecular Crystals and Liquid Crystals, 508:1, 163/[525]-172/[534], DOI: 10.1080/15421400903060557

To link to this article: http://dx.doi.org/10.1080/15421400903060557

Mol. Cryst. Liq. Cryst., Vol. 508, pp. 163/[525]–172/[534], 2009
Copyright © Taylor & Francis Group, LLC
ISSN: 1542-1406 print/1563-5287 online
DOI: 10.1080/15421400903060557

Synthesis and Physico-Chemical Properties for 2-Oxochromen-6-yl 4-(4-Alkoxyphenylazo)benzoates

Yuki Morita, Hiroshi Uemura, Kentaro Shimoi, Kazuo Kasatani, and Hiroaki Okamoto
Department of Advanced Materials Science and Engineering, Faculty of Engineering, Yamaguchi University, Ube, Yamaguchi, Japan

This paper describes the preparation and thermal properties for homologous series of 2-oxochromen-6-yl 4-(4-alkoxyphenylazo)benzoates (compounds **1**-*n). Compounds* **1**-*n show nematic phase exclusively, where the nematic–isotropic phase transition temperatures are between 293°C for* **1**–*4 and 256°C for* **1**–*8. Interestingly, compound* **1**–*8 exhibits smectic A and re-entrant nematic phases in addition to the nematic one. The smectic A phase are characterized using a small angle X-ray diffraction study, indicating the smectic A phase has a partially bilayer molecular arrangement.*

Keywords: re-entrant nematic phase; smectic A phase; synthesis; X-ray diffraction study

INTRODUCTION

It is well known that liquid crystal materials incorporating strongly polar terminal groups such as cyano and/or nitro group exhibit interesting mesomorphic behavior, including a re-entrant nematic and several smectic phases, where the large dipole moment along to the longitudinal direction of the molecule is supposed to play an important role [1].

This work is supported by Industrial Technology Research Grant Program in 2006 from New Energy and Industrial Technology Development Organization (NEDO) of Japan, and Grant-in-Aids for Young Scientists (B) from the Ministry of Education, Culture, Sports, Science and Technology of Japan.

Address correspondence to Hiroaki Okamoto, Department of Advanced Materials Science and Engineering, Faculty of Eng., Yamaguchi University, Tokiwadai 2557, Ube, Yamaguchi 755-8611, Japan. E-mail: oka-moto@po.cc.yamaguchi-u.ac.jp

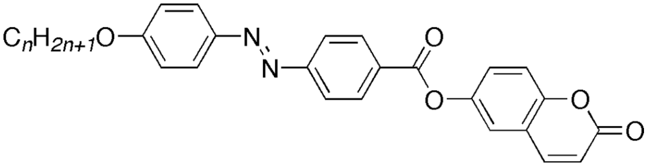

FIGURE 1 Chemical structure for compounds **1**-n.

Recently, several liquid crystal materials having a terminal carbonyl group such as lactone and cyclic carbonate groups were prepared and it has been clarified that the terminal carbonyl groups affect the mesomorphic and dielectric properties differently from the terminal cyano and nitro groups. In earlier papers [2–6], for example, we have reported that a terminal 1,3-dioxan-2-one and the related skeletons affect their mesomorphic, physical, and dielectric properties. Furthermore, we have also investigated some liquid crystal materials having a 2-oxo-chromen (coumarin) skeleton at the terminal position of the molecule and their benzoate system shows not only mesomorphic properties but also gelation one [7,8].

This paper describes the preparation and the thermal properties of homologous series of 2-oxochromen-6-yl 4-(4-alkoxyphenylazo) benzoates (compounds **1**-n) as shown in Figure 1. The experimental results are discussed in terms of the molecular structure.

EXPERIMENTAL

Materials

Compounds **1**-n were synthesized according to Scheme 1, where compounds **1**-n and synthetic intermediates were characterized by means of IR and ^{1}H NMR spectra and the results are as follows.

Physical data for compounds **1**-n are as follows.

IR and ^{1}H NMR spectra for compound **1**-4: IR (KBr disc); $\nu = 1242.2$, 1597.1, 1734.0, 1743.7, and 2960.7 cm^{-1}. ^{1}H NMR (CDCl$_3$); $\delta = 1.01$ (3H, t, $J = 6.5$ Hz), 1.56 (2H, six., $J = 6.5$ Hz), 1.83 (2H, qui., $J = 6.5$ Hz), 4.08 (2H, t, $J = 6.5$ Hz), 6.50 (1H, d, $J = 9.6$ Hz), 7.03 (2H, d, $J = 8.9$ Hz), 7.42 (3H, s), 7.71 (1H, d, $J = 9.6$ Hz), 7.97 (2H, d, $J = 8.9$ Hz), 7.99 (2H, d, $J = 8.9$ Hz), and 8.33 (2H, d, $J = 8.6$ Hz) ppm.

IR and ^{1}H NMR spectra for compound **1**–5: IR (KBr disc); $\nu = 1138.0$, 1259.5, 1735.9, and 2956.9 cm^{-1}. ^{1}H NMR (CDCl$_3$); $\delta = 0.96$ (3H, t, $J = 6.9$ Hz), 1.38–1.54 (4H, m), 1.85 (2H, qui., $J = 6.9$ Hz), 4.07 (2H, t, $J = 6.9$ Hz), 6.50 (1H, d, $J = 9.6$ Hz), 7.03

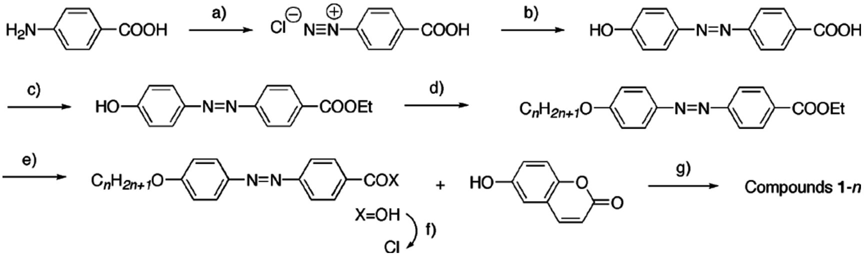

SCHEME 1 Synthetic scheme for compounds **1**-*n*; Reagents and conditions; a) $NaNO_2$, 1 M HCl, b) Phenol in 6 M NaOH, then poured into 2 M HCl, c) H_2SO_4, EtOH, reflux, d) $C_nH_{2n+1}Br$, K_2CO_3, 3-pentanone, reflux, e) 6 M NaOH, then poured into 2 M HCl, f) $SOCl_2$ 70°C, g) 6-hydroxycoumarine, pyridine, 70°C.

(2H, d, $J = 8.9$ Hz), 7.42 (3H, s), 7.72 (1H, d, $J = 9.6$ Hz), 7.97 (2H, d, $J = 8.9$ Hz), 7.99 (2H, d, $J = 8.9$ Hz), and 8.32 (2H, d, $J = 8.6$ Hz) ppm.

IR and ^{1}H NMR spectra for compound **1**–6: IR (KBr disc); $\nu = 1139.9$, 1238.3, 1720.5, and 2941.4 cm^{-1}. ^{1}H NMR ($CDCl_3$); $\delta = 0.92$ (3H, t, $J = 6.5$ Hz), 1.36–1.57 (6H. m), 1.84 (2H, qui., $J = 6.5$ Hz), 4.07 (2H, t, $J = 6.5$ Hz), 6.50 (1H, d, $J = 9.2$ Hz), 7.02 (2H, d, $J = 8.9$ Hz), 7.42 (3H, s), 7.71 (1H, d, $J = 9.6$ Hz), 7.97 (2H, d, $J = 8.9$ Hz), 7.99 (2H, d, $J = 8.9$ Hz), and 8.33 (2H, d, $J = 8.9$ Hz) ppm.

IR and ^{1}H NMR spectra for compound **1**–7: IR (KBr disc); $\nu = 1143.8$, 1290.2, 1728.2, and 2939.5 cm^{-1}. ^{1}H NMR ($CDCl_3$); $\delta = 0.91$ (3H, t, $J = 6.5$ Hz), 1.24–1.53 (8H, m), 1.84 (2H, qui., $J = 6.5$ Hz), 4.07 (2H, t, $J = 6.5$ Hz), 6.50 (1H, d, $J = 9.6$ Hz), 7.03 (2H, d, $J = 8.9$ Hz), 7.42 (3H, s), 7.71 (1H, d, $J = 9.4$ Hz), 7.97 (2H, d, $J = 8.9$ Hz), 7.99 (2H, d, $J = 8.9$ Hz), and 8.32 (2H, d, $J = 8.9$ Hz) ppm.

IR and ^{1}H NMR spectra for compound **1**–8: IR (KBr disc); $\nu = 1139.9$, 1244.1, 1734.0, 1745.6, and 2924.1 cm^{-1}. ^{1}H NMR ($CDCl_3$); $\delta = 0.90$ (3H, t, $J = 6.5$ Hz), 1.21–1.57 (10H, m), 1.84 (2H, qui., $J = 6.5$ Hz), 4.05 (2H, t, $J = 6.6$ Hz), 6.50 (1H, d, $J = 9.6$ Hz), 7.03 (2H, d, $J = 8.9$ Hz), 7.42 (3H, s), 7.72 (1H, d, $J = 9.6$ Hz), 7.97 (2H, d, $J = 8.6$ Hz), 7.99 (2H, d, $J = 8.6$ Hz), and 8.33 (2H, d, $J = 8.6$ Hz) ppm.

METHOD

The transition temperatures and latent heats were determined using a Seiko SSC-5200 DSC, where indium (99.9%) was used as a calibration standard (mp = 156.6°C, 28.4 J/g). The DSC thermogram was operated at a heating or cooling rate of 5°C min^{-1}. The mesophases were characterized using a Nikon POH polarizing microscope fitted with a Mettler thermo-control system (FP-900). The homogeneous and homeotropic alignments between glass surfaces were achieved by treatment of glass plates with polyimide (Tore SP-810) and cetyltrimethyl ammonium bromide, respectively. ^{1}H NMR spectra were measured using a JEOL EX-270 spectrometer, where tetramethylsilane was used as an internal standard. IR spectra were recorded with a Shimadzu Prestige-21 infrared spectrometer. The purity of the materials was checked by HPLC and DSC thermograms using a 'DSCPURITY' program (SII instrument) instead of elemental analysis.

X-ray diffraction experiments for the SmA phase were performed using a Rigaku RINT 2200 diffractometer, where CuKα ($\lambda = 1.541$ Å) was used as an X-ray source. The reflection angle was calibrated by a comparison of both right and left angles. The temperature was controlled using a Rigaku PTC-20A controller. The samples were heated to the re-entarant nematic phase and filled into the quartz capillary (1.0 mmϕ). The sample was oriented by a constant magnetic field (480 G) and the measurements were carried out during the heating process.

The molecular lengths were calculated by a semi-empirical molecular orbital calculation, where minimization of the total energy was achieved by an AM1 method [9].

RESULTS AND DISCUSSION

Mesomorphic properties for compounds **1**-*n* were determined by means of DSC measurements and polarized microscope observations.

Compound **1**–7 shows endotherms at 124°C and 263°C corresponding to the melting and mesophase–isotropic (I) phase transition phenomena on heating process. The molten material showed a small exotherm at 261°C due to the phase transition during a cooling process. The formed texture is shown in Figure 2. The mesophase shows a typical Schlieren texture under polarized microscope observation (see Fig. 2). Therefore, the mesophase is assigned to be a nematic (N) phase.

For compound **1**–8, a typical focal conic fan texture is also observed at 216°C in addition to the Schlieren one on cooling process as shown in Figure 3(a) and (b). We assume that the mesophases have an orthogonal alignment of the molecule, since the mesophases show a typical homeotropic texture (dark under a cross-polarized microscope) under a homeotropic alignment. Therefore, the mesophases are assigned to be the N and smectic A (SmA) phases, whereas analogues of compounds **1**-n, 4-methyl-7-coumaryl 4-(4-alkoxyphenylazo) benzoates, show a smectic C phase as well as the N phase [10]. Interestingly, compound **1**–8 exhibits another Schlieren texture under a homogeneous

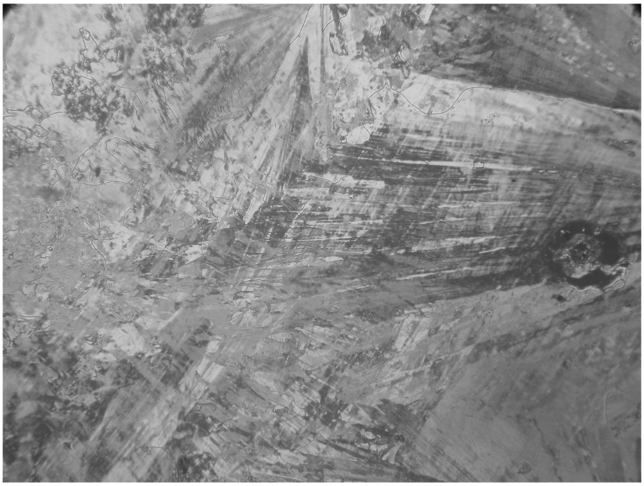

FIGURE 2 Polarized micrograph for compound **1**–7 at 255°C.

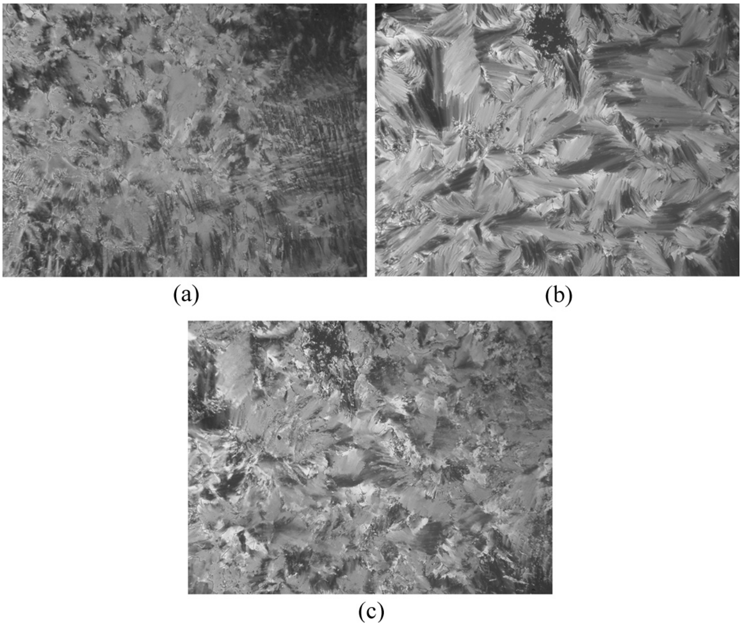

(a) (b)

(c)

FIGURE 3 Polarized micrographs for compound **1**–8: (a) nematic (N) phase (254°C), (b) smectic A (SmA) phase (202°C), (c) re-entrant nematic (N_{re}) phase (132°C).

alignment surface at 149°C on cooling of the SmA phase as can be seen in Figure 3(c). The mesophase below the SmA phase is assigned to be a re-entrant N (N_{re}) phase as a result.

The transition temperatures for **1**-n are summarized in Table 1 and plotted against the carbon numbers (n) in the alkoxy chain (Fig. 4).

The N–I transition temperatures for **1**-n decrease on ascending the homologues, while the melting points are almost independent of the carbon numbers (n). Compound **1**–8 has the phase sequence of crystal (C)–N_{re}–SmA–N–I, while compound **1**–7 C–N–I as described before.

It is known that the re-entrant phenomenon in liquid crystals was frequently found in cyano and nitro compounds [11], which is so-called "polar liquid crystals". To the best of our knowledge, the appearance of the N_{re} phase of compound **1**–8 is a first example for a single liquid crystal material having a carbonyl group at the terminal position of the molecules, suggesting the introduction of the coumarin skeleton gives a polar nature in liquid crystal materials.

The SmA phase was also characterized by means of X-ray diffraction measurements, and the X-ray profile for compound **1**–8 at 160°C is shown in Figure 5.

The reflection peak arising from a smectic layer was observed at $2\theta = 2.39°$ (36.9 Å), on the other hand, there was no apparent peak in the wide-angle region. The results also support the characterization of the SmA phase of compound **1**–8.

The phase transition behavior and layer structures of the SmA phase were further characterized using small angle X-ray diffraction measurements in variable temperatures as shown in Figure 6.

The diffraction peak appeared obviously at 160°C on heating process, while there is no apparent peak at 150°C. The intensity of

TABLE 1 Transition Temperatures for Compounds **1**-n

Compounds **1**-n	Transition temperature (°C)								
n	C		N_{re}		SmA		N		I
4	●	136	–		–		●	293	●
5	●	130	–		–		●	280	●
6	●	119	–		–		●	272	●
7	●	124	–		–		●	263	●
8	●	125	●	149	●	216	●	256	●

C, N_{re}, SmA, N and I indicate crystal, re-entrant nematic, smectic A, nematic and isotropic phases, respectively.

*Latent heats for N_{re} – SmA and SmA – N transitions could not be observed by DSC measurements.

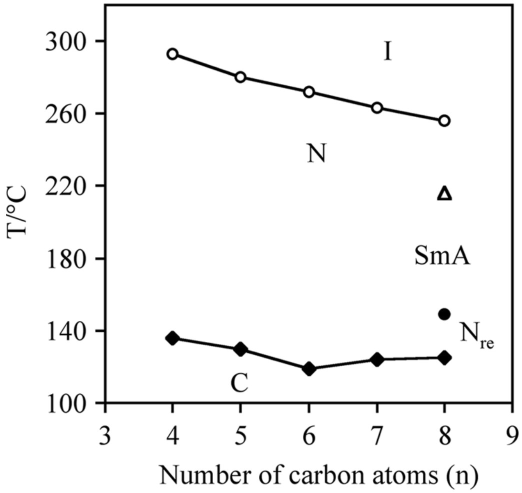

FIGURE 4 Plots of transition temperatures against the number of the carbon atoms (n) for compounds **1**-n; Diamonds, circle (filled), triangle and circles (open) denote melting points, N_{re}–SmA, SmA–N and N–I transition temperatures, respectively.

diffraction peaks becomes large and sharp with increasing the temperatures, suggesting the order of the molecular arrangements arise in the SmA phase. These results also support the existence of the N_{re} phase below the SmA one.

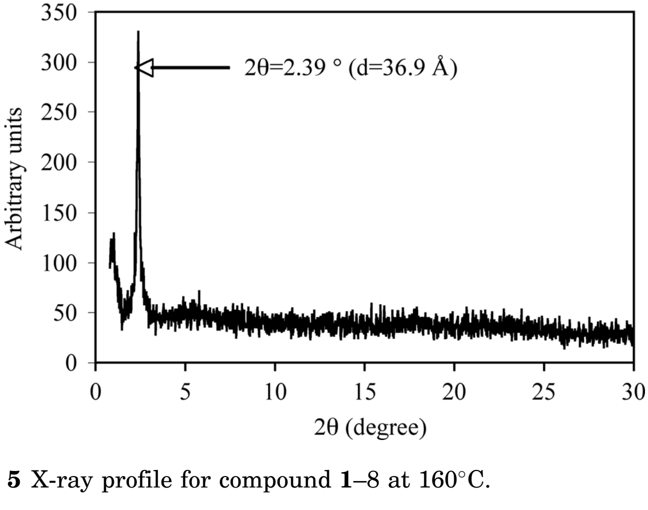

FIGURE 5 X-ray profile for compound **1**–8 at 160°C.

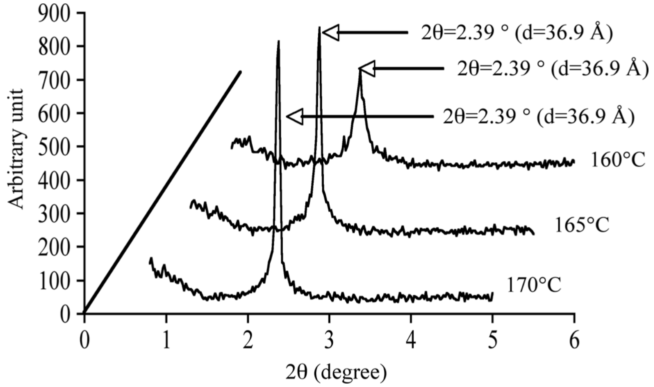

FIGURE 6 X-ray profiles for compound **1**–8 at (a) 160°C, (b) 165°C, (c) 170°C.

The diffraction angles arising from the SmA layer are observed at $2\theta = 2.39°$ (d = 36.9 Å) and independent of the temperature between 160°C and 170°C.

In order to consider the molecular arrangements in the SmA phase, the molecular structure and dipole moment of compound **1**–8 were estimated using a semi-empirical molecular calculation (AM1 method) [9] as shown in Figure 7.

The molecular length (l) of compound **1**–8 is calculated to be 30.8 Å, which is 6.1 Å shorter than the layer spacing (36.9 Å) of the SmA phase, so that the SmA phase is assigned to be so-called "$\mathrm{SmA_d}$" phase, which is frequently observed in polar liquid crystal materials. The characterization of the $\mathrm{SmA_d}$ phase is also supported by the semi-empirical molecular orbital calculation, in which compound **1**–8 has a large dipole moment (8.5 D) mainly arising from the terminal coumarin skeleton and should have a polar liquid crystal nature. On the other hand, the length of the coumarin skeleton for compound

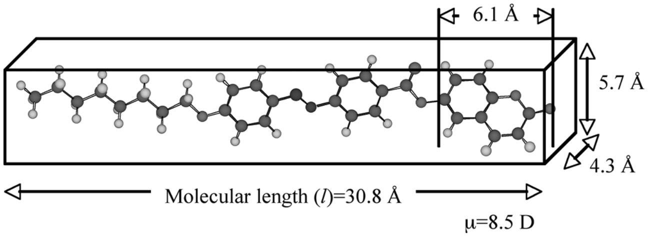

FIGURE 7 Molecular structure and dipole moment for compound **1**–8, calculated by a semi-empirical molecular orbital calculation (AM1).

1–8 is calculated to be 6.1 Å, agreed with the difference of the layer spacing (*d*) and molecular length (*l*).

These results suggest that there are two possibilities for the molecular arrangements in the $\mathrm{SmA_d}$ phase as shown in Figure 8.

In Figure 8(a), coumarin skeletons are gathered around the smectic layer boundary and the parts of the compound **1**–8 including the alkyl chain are arranged in the center of the smectic layers. In Figure 8(b), on the other hand, coumarin skeletons are arranged in the center of the smectic layer and some parts of the terminal alkyl chain are gathered around the smectic layer boundary, which is the conventional molecular arrangement in the $\mathrm{SmA_d}$ phase.

In our earlier papers, some liquid crystal materials have unconventional molecular arrangements, because of the electrostatic and steric effects of the terminal groups [12–19].

It seems to be difficult to clarify the molecular arrangements in the $\mathrm{SmA_d}$ phase since there are not enough experimental data at present.

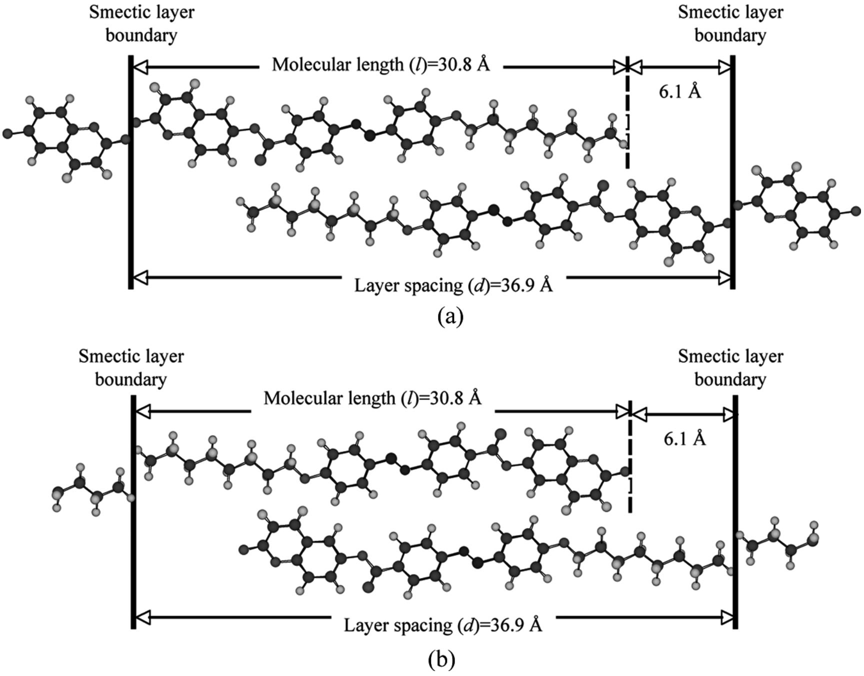

FIGURE 8 Possible molecular arrangements in the SmA phase for compound **1**–8: coumarin groups are arranged around (a) the smectic layer boundary and (b) the center of the smectic layer.

However, the re-entrant phenomena for compound **1**–8 and the gelation properties for the corresponding benzoate systems [7,8] might have some relationship in molecular arrangement.

Further examination is now underway, and the results will be published elsewhere.

REFERENCES

[1] Gray, G. W. & Goodby, J. W. (1984). *Smectic Liquid Crystals*, Heyden & Son Inc.: Philadelphia, 134.

[2] Okamoto, H., Okamoto, T., & Takenaka, S. (2000). *Chem. Lett.*, 1040.

[3] Okamoto, H., Okamoto, T., Petrov, V. F., & Takenaka, S. (2001). *Mol. Cryst. Liq. Cryst.*, *364*, 719–725.

[4] Morita, Y., Tasaka, T., Kabu, K., Okamoto, H., & Takenaka, S. (2004). *Trans. Mater. Res. Soc. Jpn*, *29*, 831.

[5] Morita, Y., Yamaguchi, R., Okamoto, H., & Takenaka, S. (2005). *Mol. Cryst. Liq. Cryst.*, *439*, 2075.

[6] Morita, Y., Zhang, F., Tasaka, T., Yamaguchi, R., Okamoto, H., & Takenaka, S. (2006). *Bull. Chem. Soc. Jpn*, *79*, 163.

[7] Morita, Y., Kawabe, K., Zhang, F., Okamoto, H., Takenaka, S., & Kita, H. (2005). *Chem. Lett.*, *34*, 1650.

[8] Zhang, F., Morita, Y., Kawabe, K., Tasaka, T., Okamoto, H., Takenaka, S., & Kita, H. (2006). *Inter. J. Nanoscience*, *5*, 781.

[9] Dewar, M. J. S., Zoebisch, E. G., Healy, E. F., & Steward, J. J. P. (1985). *J. Am. Chem. Soc.*, *107*, 3902.

[10] Dave, J. S., Menon, M. R., & Patel, P. R. (2002). *Liquid Crystals*, *29*, 543.

[11] Cladis, P. E. (1999). In *Physical Properties of Liquid Crystals*, Demus, D., Goodby, J., Gray, G. W., Spiess, H.-W., & Vill, V. (Eds.), chapter 6.4, WILY-VCH.

[12] Duan, M., Okamoto, H., Petrov, V. F., & Takenaka, S. (1998). *Bull. Chem. Soc. Jpn.*, *71*, 2735.

[13] Okamoto, H., Petrov, V. F., & Takenaka, S. (1999). *Liquid Crystals*, *26*, 691.

[14] Duan, M., Okamoto, H., Petrov, V. F., & Takenaka, S. (1999). *Liquid Crystals*, *26*, 737.

[15] Duan, M., Tasaka, T., Okamoto, H., Petrov, V. F., & Takenaka, S. (2000). *Liquid Crystals*, *27*, 1195.

[16] Kimoto, K., Duan, M., Okamoto, H., Petrov, V. F., Hori, K., & Takenaka, S. (2001). *Mol. Cryst. Liq. Cryst.*, *364*, 733.

[17] Tasaka, T., Petrov, V. F., Okamoto, H., Morita, Y., Suetake, K., & Takenaka, S. (2002). *Liquid Crystals*, *29*, 1311.

[18] Tasaka, T., Takenaka, S., Kabu, K., Morita, Y., & Okamoto, H. (2002). *Ferroelectrics*, *276*, 83.

[19] Tasaka, T., Okamoto, H., Morita, Y., Kasatani, K., & Takenaka, S. (2003). *Liquid Crystals*, *30*, 961.